

近紅外光感測器用之高靈敏度共軛高分子/奈米顆粒複合材料
**High Sensitivity conjugated polymer/ nanoparticle Nanocomposite
for Near IR Sensor Applications**

計畫類別： 個別型計畫 整合型計畫

計畫編號：NSC 97-2221-E-009-006-MY3

執行期間：2008年08月01日至2009年07月31日

計畫主持人：韋光華 教授

共同主持人：

計畫參與人員：郭芝吟、陳璽夷、許毓倩、林惠妮

成果報告類型(依經費核定清單規定繳交)： 精簡報告 完整報告

本成果報告包括以下應繳交之附件：

- 赴國外出差或研習心得報告一份
- 赴大陸地區出差或研習心得報告一份
- 出席國際學術會議心得報告及發表之論文各一份
- 國際合作研究計畫國外研究報告書一份

處理方式：除產學合作研究計畫、提升產業技術及人才培育研究計畫、
列管計畫及下列情形者外，得立即公開查詢

涉及專利或其他智慧財產權， 一年 二年後可公開查詢

執行單位：國立交通大學材料科學與工程學系

中文摘要

keyword: 表面電漿共振效應、核殼顆粒、共軛高分子、紅外光偵測器

本計劃的主要目的在於發展以延長共軛高分子/奈米顆粒形成之奈米複合材料製造高靈敏度近紅外光偵測器之元件與特性探討，工作範圍包含了合成具有能隙小於 1.3 電子伏特且具紅外光吸收之共軛高分子，並利用靜電組裝法制備金/二氧化矽核殼顆粒與膠體化學方法來製造金奈米棒與 PbSe 量子點奈米顆粒。主要構思為利用具表面電漿共振效應之金奈米顆粒棒及具紅外光吸收之 PbSe 量子點奈米顆粒與所合成之高分子結合形成共軛高分子/奈米複合材料，藉此來提升紅外光感測器之靈敏度與熱穩定性。在聚合物材料的合成方面，主要以共軛性高分子為主幹，連結染料分子或無機粒子以增加紅外光吸收範圍。

最後我們期望將金/二氧化矽核殼顆粒、金奈米棒或 PbSe 量子點奈米顆粒與高分子結合形成共軛高分子/奈米複合材料，再利用濕式製程技術如 spin casting、ink jet printing、screen printing 以及 micro-molding 塗佈在電極上並製成元件，並測量其元件特性。

英文摘要

keyword: surface plasmon resonance effect、core shell、conjugation polymer、IR sensor

In the proposed research, we plan to fabricate high sensitivity near IR sensor with nanoparticle/ conjugation polymer nanocomposites and analyzing the characterization of the devices. The work for this project involves synthesizing conjugation polymer which have low band gap (less than 1.3 eV) and IR absorption. Additionally, we plan to synthesize gold nanorods and PbSe quantum dots by colloid chemical method. The main objective of this project is to utilize gold nanorods with surface plasmon resonance effect and IR-absorption PbSe nanoparticles, then to combine with conjugation polymer to enhance sensitivity and thermal stability of IR sensor consist of nanoparticle/ conjugation polymer nanocomposites.

For the polymer synthesizing, a series of polymer materials with high absorption coefficient and broad infrared absorption spectrum. The main strategy of the project is to incorporate dye molecules or inorganic particles onto conjugated polymer backbone via physical or chemical absorption to increase the range of IR absorption spectrum. Meanwhile, the effect of composition, dye structure, the shape, size and content of inorganic particles on the characteristics of absorption spectrum of materials will be explored.

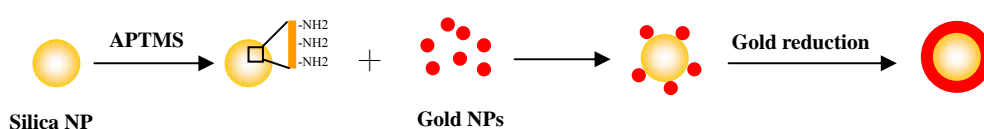
We plan to use synthesized conjugation polymer, which have low band gap (less than 1.3 eV) and nanoparticles by this project to form nanocomposites for near IR sensor device fabrication and measure the characterization.

A. Synthesis of Plasmonic Active titanium dioxide/gold and silica/gold core-shell structured nanoparticles (NPs).

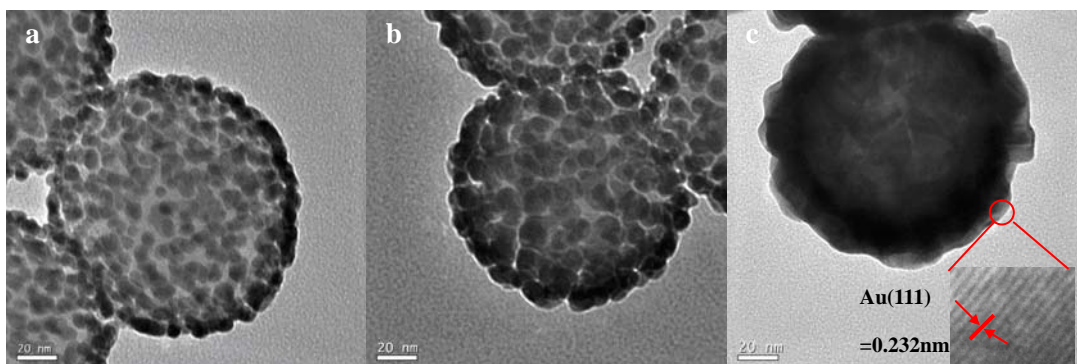
Metal nanoshells, consisting of a dielectric core with a metallic shell of nanometer thickness, are a new type of composite nanoparticles that have “designed in” optical resonance-by varying the relative dimensions of the core and shell, the optical resonance of these nanoparticles can be varied over hundreds of nanometers in wavelength, across the visible and into the infrared region of the spectrum. We report a general approach to the making of metal nanoshell composite nanoparticles based on molecular self-assembly and colloid reduction chemistry.¹

Metal nanoshells have been fabricated by a method.² Silica nanoparticles were grown by the Stöber method,³ in which tetraethyl orthosilicate(TEOS) was reduced in NH_4OH in ethanol. The particle surface was then terminated with amine groups by reaction with aminopropyltrimethoxysilane(APTMS) in ethanol. Very small gold colloid (1–3 nm) was grown by using the method of Duff and Baiker.⁴ This colloid was aged for 2 weeks at 4°C and was then concentrated by using a rotary evaporator. Aminated silica particles were then added to the gold colloid suspension. Gold colloid adsorbs to the amine groups on the silica surface, resulting in a silica nanoparticle covered with gold colloid. Gold–silica nanoshells were then grown by reacting HAuCl_4 with the silica-colloid particles in the presence of NaBH_4 .

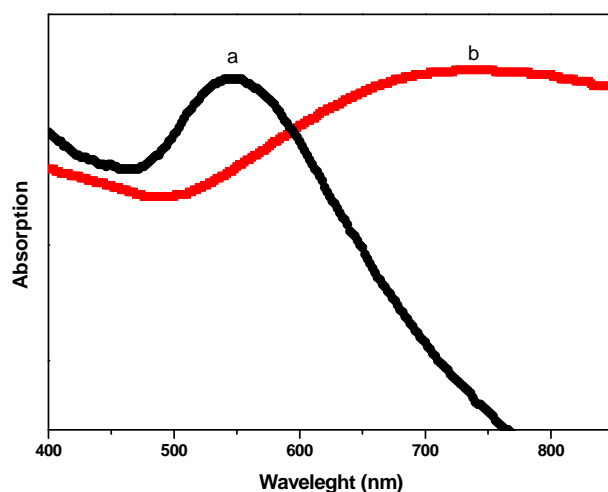
The near IR-ultraviolet-visible (NIR-UV-Vis) extinction spectra of the nanoparticles and nanoparticle assemblies were measured in solution using a Hitachi U-4100 spectrophotometer with the appropriate mixture of ethanol and water as a reference. A JEOL JEM-2010 electron microscope operating at an accelerating bias voltage of 200 kV was used to collect the TEM images. Samples for TEM were prepared on copper grids (size 200 mesh) coated with a carbon support film. Samples were prepared by placing a drop of a solution of the nanoparticles on a grid placed on filter paper and allowing the solvent to evaporate.



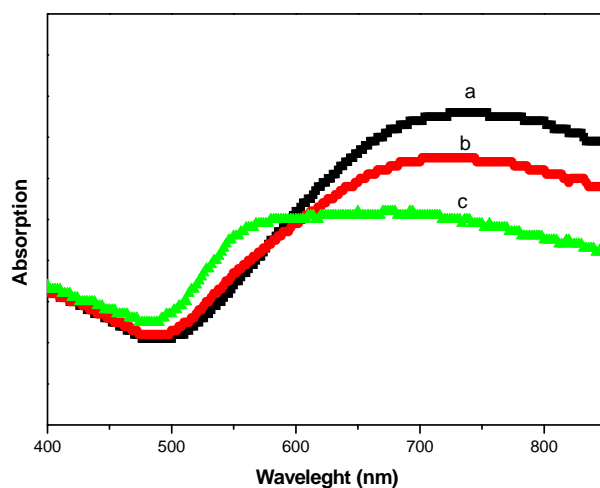
Scheme. Strategy Used To Grow a Gold Nanoshell around a Silica Nanoparticle Core



TEM images of nanoshell growth on 100 nm diameter silica dielectric nanoparticles. (a-b) Gradual growth and coalescence of gold colloid on silica nanoparticle surface. (c) Completed growth of metallic nanoshell. A nanoparticle having a silica core diameter of ~100 nm and a gold shell of 20 nm thick.



UV-vis absorbance of a) Gold NPs, b) SiO₂/Au core-shell NPs. ($\sim 150 \pm 5$ nm silica NP and gold nanoshell with a shell thickness of $\sim 20 \pm 5$ nm)



UV-vis absorbance of SiO₂/Au core-shell NPs with 150 ± 5 nm silica core and shell thickness of a) 20 ± 5 nm; (b) 22 ± 5 nm; (c) 25 ± 5 nm.

Metallic nanoshells are, in essence, versatile subwavelength optical components with the remarkable property that their surface plasmon resonance can be tuned across the visible and near-infrared spectral regions by varying the relative dimensions of their core and shell layers.

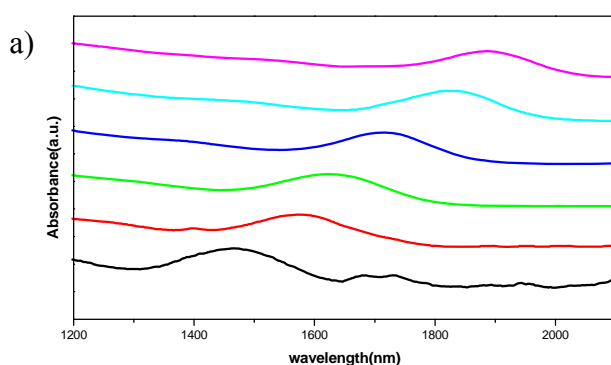
B. Synthesis of PbSe nanoparticles with Tunable Absorption in IR range

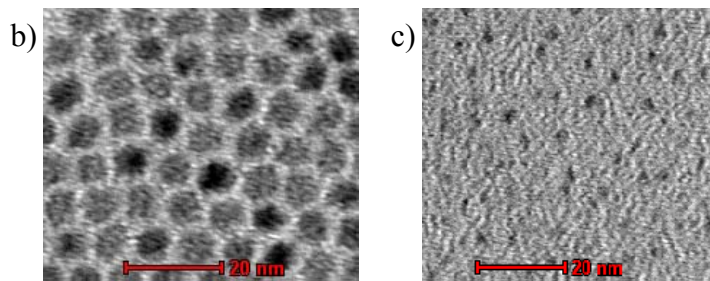
Solution-processed photovoltaics offer solar energy harvesting characterized by low cost, ease of processing, physical flexibility, and large area coverage.^{5,6} Conjugated polymers,⁷ inorganic nanocrystals (NCs),⁸ and hybrid materials⁹ have been widely investigated and optimized to this purpose. Organic solar cells have already achieved 6.5% solar conversion efficiencies.¹⁰ These devices, however, fail to harvest most of the infrared (IR) spectral region. High efficiency multijunction solar cells offer the prospect of exceeding 40% efficiency¹¹ through the inclusion of infrared-bandgap materials. In this context, infrared single-junction solar cells should be optimized for infrared power conversion efficiency rather than solar power conversion efficiency.

For double- and triple-junction solar cells, the smallest- bandgap junction optimally lies at 1320 and 1750 nm, respectively. Attempts to extend organic solar cell efficiency into the near-infrared have so far pushed the absorption onset only to 1000 nm.¹² By virtue of their size-tunable optical properties, lead salt colloidal quantum dots(CQDs) can be engineered to access the visible and the short- wavelength infrared spectral regions.¹³

PbSe semiconductor nanocrystals were synthesized in a three-neck flask equipped with condenser, magnetic stirrer, thermocouple, and heating mantle. Typically, a mixture of 0.892 g of PbO (4.00 mmol), 2.825 g of oleic acid (10.00mmol), and technological grade 1-octadecene (ODE) (the total weight was 16 g) turned colorless upon heating to around 150°C; the mixture was further heated to 180 °C. Then, 6.4 g of selenium-trioctylphosphine solution (containing 0.64 g of selenium, 8.00 mmol) was quickly injected into this hot solution; the temperature of the reaction mixture was allowed to cool to 150 °C for the growth of the PbSe semiconductor nanocrystals. All steps in the reactions were carried out under argon. The nanocrystal growth process here is continuous. It should be pointed out that ODE and oleic acid, which show strong absorption in NIR, must be removed from the original aliquots taken from the reaction flask before the absorption measurement. The aliquot was swiftly taken out and quenched by room-temperature chloroform. The chloroform solution was extracted twice with an equal volume of methanol; then the ODE phase was mixed with excess acetone to totally precipitate PbSe semiconductor nanocrystals. The precipitated PbSe semiconductor nanocrystals were redispersed in chloroform or hexane and were precipitated again by excess acetone. The purified PbSe semi- conductor nanocrystals (solid state) were finally dispersed in tetrachloroethylene for NIR absorbance and other characterizations. During the purification process, the PbSe semiconductor nanocrystals were completely recovered, and there was no size selection applied to the sample.¹⁴

The near IR-ultraviolet-visible (NIR-UV-Vis) extinction spectra of the nanoparticles and nanoparticle assemblies were measured in solution using a Hitachi U-4100 spectrophotometer with the appropriate mixture of ethanol and water as a reference. A FEI T12 electron microscope operating at an accelerating bias voltage of 120 kV was used to collect the TEM images. Samples for TEM were prepared on copper grids (size 200 mesh) coated with a carbon support film. Samples were prepared by placing a drop of a solution of the nanoparticles on a grid placed on filter paper and allowing the solvent to evaporate.





(a) Size-dependent absorption spectra of the as-prepared PbSe nanocrystals spanning the range of tunable sizes.

Transmission electron microscopy of as-synthesized oleate-capped PbSe NCs used in this investigation (b) 8.5 nm

(c) 3.5 nm.

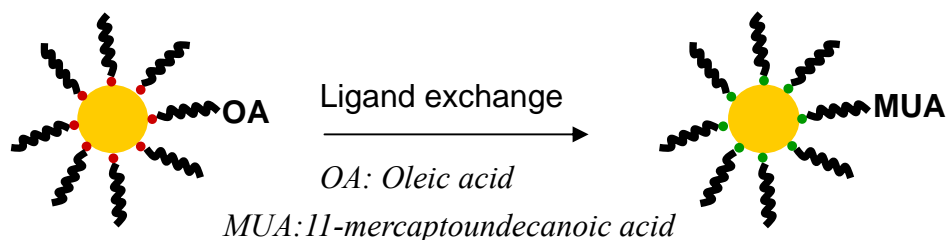
C. PbSe ligand exchange

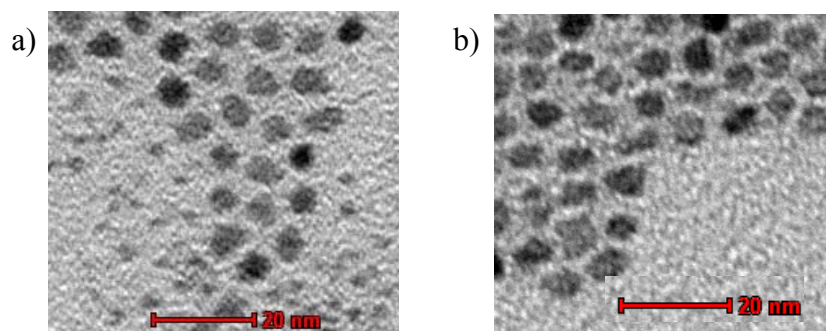
A FEI T12 electron microscope operating at an accelerating bias voltage of 120 kV was used to collect the TEM images. Samples for TEM were prepared on copper grids (size 200 mesh) coated with a carbon support film. Samples were prepared by placing a drop of a solution of the nanoparticles on a grid placed on filter paper and allowing the solvent to evaporate. Atomic force microscopy (AFM) was acquired using a DI tapping mode AFM. A JEOL JSM-6500F field emission scanning electron microscope (SEM) was used to image the NCs.

a. Water-Soluble PbSe QD

We describe the typical synthesis of water-soluble PbSe QDs wrapped with 11-mercaptopundecanoic acid (MUA, 95%), which follows a process reported for water-soluble CdTe QDs.¹⁵ To prepare negatively charged MUA-capped PbS QDs, 100 μ L of PbS QDs in toluene (2.5 mg/mL) was mixed into 0.5 mL of MUA in chloroform (7 mg/mL). The mixture was shaken vigorously for about 1 min until the QDs flocculated. After flocculation, 400 μ L of NaOH in water (1.9 mg/mL, 20 mol % excess of NaOH) was added to the suspension, resulting in a two-phase system, aqueous and chloroform phases. After shaking and centrifuging the solution, the QDs were transferred into the water phase. All free carboxylic acid groups convert to their salt forms (COO^-Na^+). Therefore, the surfaces of the QDs are expected to be negatively charged.

The as-synthesized NCs (Figure a) were capped with ~ 2.5 nm oleate ligands. The oleate ligands were replaced with shorter 11-mercaptopundecanoic acid ligand (~ 1.1 nm, Figure b) and with a solution-phase ligand exchange. Ligand exchange decreases the NC spacing.





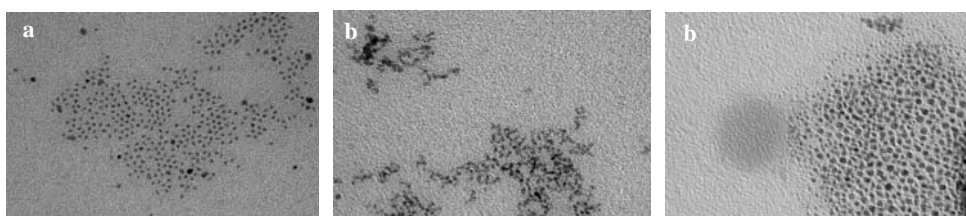
TEM image of (a)PbSe NCs in CHCl_3 ; (b)Water soluble PbSe NCs.

b. Post-Synthetic Ligand Exchange

PbS, PbSe nanocrystals capped with oleic acid were found to be insulating. The, 2.5nm-long ligand inhibited carrier transport among the nanocrystals. To improve carrier mobility, we used a post-synthetic ligand exchange to replace oleic acid with shorter ligand.^{16,17}

A. PbSe solution exchange

Nanocrystal ligand exchanges were performed in a N_2 glovebox (<20 ppm O_2). One milliliter of oleic acid-capped nanocrystals was dispensed into a 15 mL test tube. One milliliter of butylamine was added and the solution mixed with a pipet. After ~1 min, the nanocrystals were precipitated by adding 12 mL of methanol. The nanocrystals were recovered by centrifuging for 1 min, pouring off the supernatant, and drying under vacuum for 5 min. Butylamine was added to the dried nanocrystals to give a solution concentration of 100 mg/mL, and the solution was mixed vigorously until the nanocrystals had completely re-dispersed (~5 min). The nanocrystals were then precipitated with 12 mL of isopropanol, centrifuged 1 min, the supernatant decanted, and the remaining nanocrystals dried under vacuum again (5 min). The dried nanocrystals were completely dispersed to 100 mg/mL in butylamine again, and then precipitated with minimal isopropanol (approximately a 1:1 ratio by volume). After centrifuging, the lightly colored supernatant was poured off and the nanocrystals were dried by hand pumping 50 times with a pipet and large bulb. The dried nanocrystals were then dispersed in octane to 150 mg/mL.

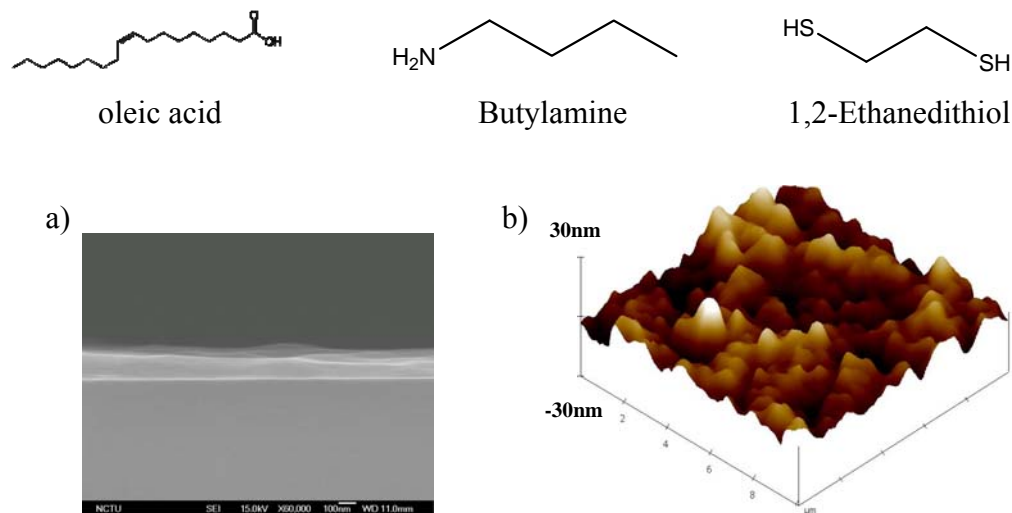


TEM images of (a)as-synthesized, (b)worm-like butylamine-solution exchanged, and (c) ovum-like octylamine-solution- exchanged PbSe nanoparticles. Scale bar is 20nm.

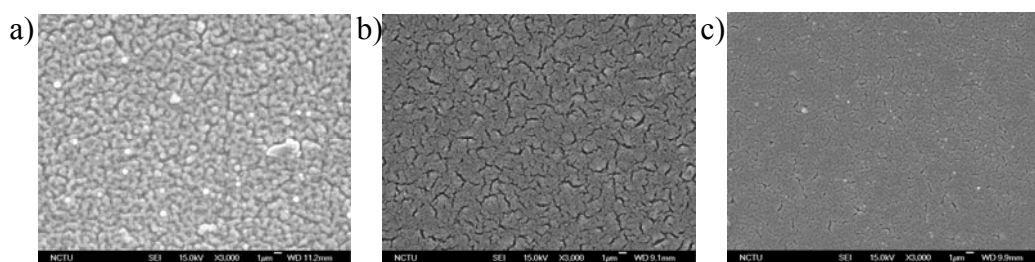
The as-synthesized NCs were capped with ~2 nm oleate ligands. The oleate ligands were replaced with shorter butylamine ligand(~0.7nm) and octylamine ligands (~1 nm) with a solution-phase ligand exchange.

B. PbSe film treated with shorter ligand

PbSe NC films were spin cast from an octane solution with a concentration of 100 mg mL⁻¹ (10 s @ 900 rpm, then 15 s @ 1100 rpm), yielding 200-nm-thick NC films with a peak-to-valley roughness of ± 25 nm. (Figure b) PbSe NC films were immersed in 3-5 mL of butylamine (C₄H₉NH₂), or 1,2-Ethanedithiol (SHC₂H₄SH) solutions in capped glass vials with occasional gentle agitation, also air-free. After a prescribed soak time (usually 24 h), the samples were carefully removed from the vials, washed with clean solvent, and allowed to dry in the glovebox.



Initial Oleated-PbSe NC thin film (a) SEM cross section images of PbSe NCs films on glass substrates. NCs with $\lambda_{\text{exciton}}=1800$ nm were used for these images. (b) AFM morphology and average roughness of studied PbSe nanocrystal films spin-cast on clean glass surfaces.



Plan-view SEM images of PbSe NCs films on silicon substrates as a function of chemical treatment.

(a) Initial Oleated-PbSe NC thin film; (b) film treated with butylamine; (c) 1,2-ethanedithiol solutions. NCs with $\lambda_{\text{exciton}}=1800$ nm were used for these images. Scale bar is 1 μm .

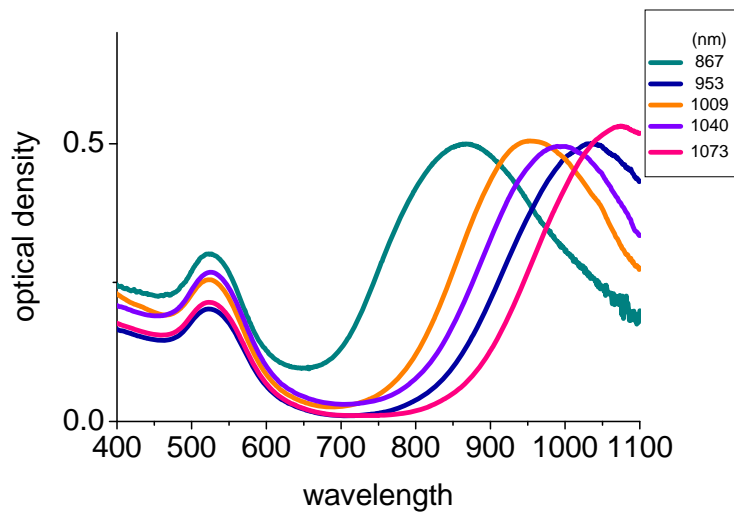
Treatments in butylamine and 1,2-ethanedithiol in acetonitrile cause little change in the gross morphology of the films. The chemical treatments remove the most oleate and result in the largest decrease in NC spacing. Post-treatment SEM images show varying degrees of film cracking as a result of oleate loss. In contrast, butylamine treatments result in extensive film cracking, less interconnected cracks than 1,2-ethanedithiol, which is consistent with its smaller degree of oleate loss. Solution concentration and time of chemical treatments can control the degree of oleate loss.

D. Synthesis of gold nanorods (NRs) and colloidal PbS NPs

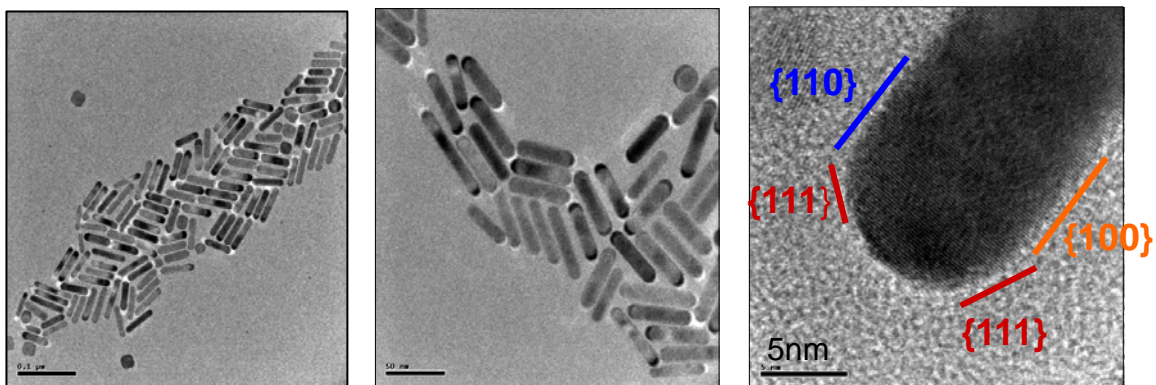
gold nanorods (NRs)

We used amphiphilic surfactants to synthesize gold nanorods that have aspect ratio about 20 and

exhibit plasmonic peaks at 497nm, due to the short axis, and at 2400nm, due to the long axis. The optical properties of these nanorods agree to the theoretical predication quite well. The yield of these gold nanorods is about 85%, and they possessed face-centered cubic crystal structure.



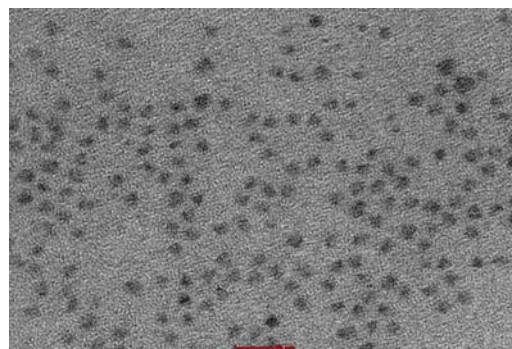
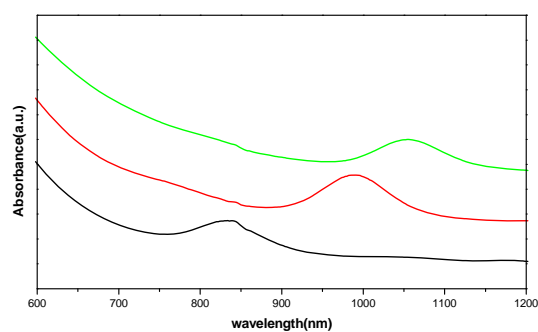
Gold NRs have particularly size-dependent optical properties, owning transverse and longitudinal surface plasma absorption.



Our gold nanorods is FCC structure

PbS NPs

A typical synthesis of PbS nanocrystals with an excitonic peak between 800 nm and 1200nm involved injection of 2.0 mmol bis(trimethylsilyl)sulphide) into a reaction flask containing 4.0 mmol lead oxide (0.9 g), 9.5 mmol oleic acid(2.67 g) and 18.8 mmol octadecene (4.73 g) at 80°C. After the injection, the reaction was quenched by moving the flask to an ice-water bath. The synthesis was carried out under inert conditions using a Schlenk line. The final PbS oleatecapped nanocrystals were isolated from any remaining starting materials and side products by precipitating with acetone. The precipitate was then re-dissolved in toluene and precipitated again with acetone.



Size-dependent absorption spectra(830nm-1060nm) of the as-prepared PbS nanocrystals spanning the range of tunable sizes. TEM image of ~4nm PbS NCs. (scale bar is 10nm)

Referece

1. S. J. Oldenburg, R. D. Averitt, S. L. Westcott, N. J. Halas *Chem. Phys. Lett.* 288, 243, **1998**.
2. K. U. Köhrmann, M. S. Michel, J. Gaa, E. Marlinghaus, P. Alken *J. Urol.* 167, 2397, **2002**.
3. W. Stöber, A. Fink *J. Colloid Interface Sci.* 26, 62, **1968**.
4. D. G. Duff, A. Baiker *Langmuir* 9, 2301, **1993**.
5. H. Hoppe, N. S. Sariciftci *J. Mater. Res.*, 19, 1924, **2004**.
6. E. H. Sargent *Adv. Mater.*, 17, 515, **2005**.
7. K. Kim, J. Liu, M. A. G. Namboothiry, D. L. Carroll *Appl. Phys. Lett.*, 90, 163511, **2007**.
8. Gur, I.; Fromer, N. A.; Geier, M. L.; Alivisatos, A. P. *Science* **2005**, 310, 462–465.
9. I. Gur, N. A. Fromer, C. Chen, A. G. Kanaras, A. P. Alivisatos *Nano Lett.*, 7, 409, **2007**.
10. J. Y. Kim, K. Lee, N. E. Coates, D. Moses, T. Nguyen, M. Dante, A. J. Heeger *Science*, 317, 222, **2007**.
11. A. Marti, G. L. Araujo *Sol. Energy Mater. Sol. Cells* , 43, 203, **1996**.
12. Wienk, M. M.; Turbiez, M. G. R.; Struijk, M. P.; Fonrodona, M.; Janssen, R. A. J. *Appl. Phys. Lett.* **2006**, 88, 153511.
13. F. Wise *Acc. Chem. Res.*, 33, 773, **2000**.
14. W. W. Yu, J. C. Falkner, B. S. Shih, V. L. Colvin *Chem. Mater.* , 16, 3318, **2004**.
15. S. F. Wuister, I. Swart, F. van Driel, S. G. Hickey, C. D. Donega *Nano Lett.*, 3 , 503, **2003**.
16. G. Konstantatos, I. Howard, A. Fischer, S. Hoogland, J. Clifford, E. Klem, L. Levina, E. H. Sargent *Nature* , 442, 180, **2006**.
17. J. M. Luther, M. Law, Q. Song, C. L. Perkins, M. C. Beard, A. J. Nozik *ACS Nano* ,2, 271, **2008**.
18. C. J. Brumlik, C. R. Martin *J. Am. Chem. Soc.*, 113, 3174, **1991**.
19. H. Y. Wu, W. L. Huang, M. H. Huang, *crystal growth design* , 7, 831, **2007**.